Vol. **108** (2005) *ACTA PHYSICA POLONICA A* No. 2

Proceedings of the XXI International Meeting on Radio and Microwave Spectroscopy
RAMIS 2005, Poznań-Będlewo, Poland, April 24–28, 2005

Molecular Dynamics of Tert-butyl Chloride Confined to CPG (7.4, 15.6 nm)

L. Szutkowska, B. Peplińska and S. Jurga*

Department of Macromolecular Physics, Adam Mickiewicz University
Umultowska 85, 61-614 Poznan, Poland

The paper complements our earlier NMR investigation of molecular dynamics of tert-butyl chloride restricted by geometries of the type MCM-41 and CPG by the new sizes of CPG and by differential scanning calorimetry method. We report proton and deuteron NMR lineshapes and the spin-lattice relaxation results of tert-butyl chloride in CPG of the 15.6 nm and 7.4 nm pore diameter in the temperature range 70 K $\leq T \leq$ 292 K. The bulk-like component of the confined tert-butyl chloride, in temperatures corresponding to phase III, is interpreted as a composition of two dynamically different subphases. The parameters of motions of both subphases are derived. The tert-butyl group motion in both subphases is more restricted than in the bulk tert-butyl chloride, although the activation energies are lower. Differential scanning calorimetry was used to determine temperatures of the phase transitions (140 K $\leq T \leq$ 292 K). The results show that the depression of the phase transition temperature is pore size dependent and that the confinement has less influence on transition to the plastic phase than on the freezing and on the solid II – solid III transition.

PACS numbers: 76.60.Es, 81.05.Rm, 33.15.Vb, 33.20.Bx, 68.35.Rh

1. Introduction

A variety of porous systems with different properties, mean pore sizes and distributions, connectivities and dimensionalities are now available and provide an opportunity to study confinement, finite size, and surface effects. Confined geometry has generated much interest in many fields of applied and fundamental research. It is well recognized that the characteristic features of the molecular motion and the thermal properties as well as the spatial structure of solids can be modified by the proximity of an interface, which provides geometrical constraints on the material [3–8]. The low dimensionality and fluid-wall interactions lead to

*corresponding author; e-mail: stjurga@main.amu.edu.pl

the formation of a highly defective nature of the crystallites or pseudo-liquid within the porous medium. As a consequence, in comparing to bulk sample in the higher temperatures decreasing mobility of the liquid and increased rotational mobility in the crystalline phases are observed [9, 10]. According to the Gibbs–Thomson equation, the observed depression of the transition temperatures is inversely proportional to the pore size [11]. This equation does not hold for the narrowest pores due to surface heterogeneity and finite size effects. Below the critical size, which depends on the properties of the confined fluid, the freezing does not occur at all [12, 13].

The relative influence of topology of the confining matrix and fluid-wall interactions are difficult to separate. To disentangle all parameters, systematic studies with adequate surface, topology and pore size modifications are needed. The tert-butyl cloride (TBC) is particularly well suited to such studies because of an interesting and well-documented phase diagram and internal dynamics [14–17]. The interaction of TBC with the surface of CPG is non-specific, so that the features studied, such as the changes in transition temperatures and molecular motion should reflect the properties of the small size crystals rather than specific interactions between TBC molecules and silica. This effect is particularly clear in the case of small pore diameter like the CPG of 7.4 nm, because of a relatively large S/V ratio, where a large fraction of confining molecules experience direct interactions with pore walls and large compressive stress. A combination of the thermal and dynamical methods is a valuable approach to investigation of molecular interactions within the constrained geometry of the surrounding silica.

In this paper the influence of confinement on the molecular dynamics and temperature of the phase transitions of TBC restricted by CPG of diameter 15.6 nm and 7.4 nm are studied by NMR ^{1}H and ^{2}H linewidths, lineshapes, spin-lattice relaxation times, and by differential scanning calorimetry (DSC) method.

2. Experimental

2.1. DSC measurements

A NETZSCH DSC204 Phoenix (Differential Scanning Calorimeter) was used to perform calorimetric experiments. Calibration of the equipment was performed using the phase transition temperatures of several pure materials. The DSC measurements were carried out in the range 140 K $\leq T \leq$ 292 K. The cooling rate was 2 K/min. The samples were sealed using high-pressure pans to avoid evaporation of TBC. The amount of the liquid TBC was chosen so that to fill the pores completely and keep a few percent of excess liquid outside the pores to detect the bulk and determine precisely the temperature depression.

2.2. NMR measurements

^{1}H and ^{2}H measurements were performed using a Bruker CXP-200 spectrometer with a 4.7 Tesla magnet. ^{1}H spin-lattice relaxation times were measured

with the standard $\pi - \tau - \pi/2$ inversion-recovery pulse sequence with phase cycling. Magnetization was inspected up to $5T_1$. ^{1}H spectra were obtained by the conventional quadrature FFT method. The same procedure was used to obtain ^{2}H spectra and ^{2}H T_1 relaxation data for the liquid and the solid phase I of TBC. ^{2}H measurements in the solid phases II and III of TBC were made with the $(\pi/2)_x - \tau_Q - (\pi/2)_y$ pulse sequence, and the spectra were obtained as the Fourier transform of the one half of the quadrupolar echo. The frequency independent ^{2}H spin-lattice relaxation data for the solid phases II and III were obtained from the recovery of the quadrupolar echo amplitude following the $\pi - \tau - (\pi/2)_x - \tau_Q - (\pi/2)_y$ sequence [18, 19]. The temperature of the sample was stabilized in a dynamic Oxford helium flow cryostat and was controlled by an Oxford ITC 503 controller. Lineshape simulations of the spectra were performed by standard methods [20] using the MXQET computer program.

The pore silica CPG of the pore diameter 15.6 and 7.4 nm were obtained from CPG Inc. The specific surface area measured by nitrogen adsorption equals 153 m^2/g for 7.5 nm and 91 m^2/g for 15.6 nm CPG.

The sample preparation has been described in the previous papers [1, 2].

3. Results and discussion

3.1. DSC

The DSC thermal curves of the bulk TBC (a) and TBC confined to CPG of pore diameter 15.6 nm (b) and 7.4 nm (c) are shown in Fig. 1. The DSC curves recorded on cooling the sample from room temperature to 140 K at the rate of 2 K/min reveal peaks, assigned to exothermic transitions. The curve for the bulk TBC (a) shows three peaks at 247 K, 214 K, and 182.4 K, which is in good agreement with literature values [17]. The first peak at 247 K is assigned to liquid–solid I transition, while the latter to the solid I – solid II (at 214 K) and solid II – solid III (182.4 K) transitions. The characteristic larger peak at 214 K marks the transition to the plastic phase, in which molecules are very mobile and orientationally disordered [21–23].

The thermograms (b) and (c) show the peaks of the phase transitions of the confined material and the bulk excess outside the pores. In the bulk samples, phase transition temperatures are given by the onset of the transition peak on DSC scans.

The same method cannot be used when dealing with confined material because of the broadening of the transition peaks.

The broadening of the transition may reflect the distribution of the phase transition temperatures, due to the polydispersity of porous medium [24]. Another explanation is that in the pores where crystallization occurs this process progresses gradually ("layer-by-layer" [25]) over a wide temperature range. The exact temperature of the phase transition cannot be determined, therefore we

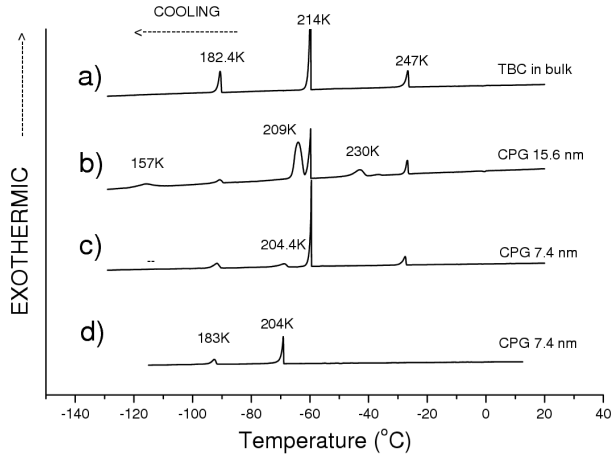

Fig. 1. Differential thermogram of (a) bulk TBC, (b) TBC confined to 15.6 nm CPG, (c) TBC confined to 7.4 nm CPG, (d) confined to 7.4 nm CPG without excess of the liquid outside the pores. The curves show the exotherms obtained on cooling.

should speak about a range of temperatures at which phase transition phenomena take place [21, 25].

In this case the temperatures of phase transitions, listed in Table I, were determined as those corresponding to the maximum of the peak.

TABLE I

Phase transition temperatures of bulk and confined TBC obtained from DSC measurements.

pore size	liquid–solid I T [K]	solid I – solid II T [K]	solid II – solid III T [K]
bulk	247	214	182
15.6 nm	230	209	157
7.4 nm	204	183	–
bulk [17]	248.4	219.4	183.1

For TBC confined to pores of diameter 7.4 nm, the phase transition solid I – solid II is observed at 183 K. The temperatures of the phase transition solid I – solid II for TBC in 7.4 nm CPG and phase transition solid II — solid III for bulk TBC are the same and the peak at 183 K, in Fig. 1c, is a superposition of two peaks. To prove this the DSC results of the sample without the excess of TBC were made and are shown in Fig. 1d. For both CPG pore sizes, the temperatures of the freezing point are lower in comparing to the bulk sample. The depression of freezing temperature increases as the pore size of CPG decreases. The temperatures of solid I – solid II transition, that is the transition to plastic

phase, observed for TBC confined to CPG with 15.6 nm as well as 7.4 nm pore diameter is also depressed, 5 K and 21 K, respectively. Similarly to the results for cyclohexane [21, 23, 25], the extent of the depression, is smaller than that of the freezing temperatures, 17 K and 43 K, respectively.

The solid II – solid III phase transition of TBC in 15.6 nm pores was detected at 157 K and the extent of the depression, 25 K, comparing to that of the freezing temperature, 17 K, is larger, like in a typical solid–solid phase transition [26, 27]. The results show that the confinement has less influence on transition to the plastic phase than on freezing and on the solid II – solid III transition.

The phase transition solid II – solid III for TBC in 7.4 nm CPG was not observed down to 140 K. It may be due to additional heterogeneity in the orientation and structure of the adsorbed layers induced in smaller pores by the radius of curvature. A crystal growing inside a pore, because of relative strong reduced size, experiences larger compressive stress, so the structure of the solid TBC is in the form of a disordered aggregate rather than in its conventional solid structure, and solid–solid transitions do not occur at all [23, 28, 29]. Probably the critical size of the crystal is required. Also, it may be argued that the number of molecules of TBC in pores with high S/V is not large enough to detect the solid II – solid III phase transitions due to the resolution of our DSC system or that temperature of the shifted phase transition has not been reached.

3.2. Spin-lattice relaxation

The ^{1}H and ^{2}H spin-lattice relaxation times as a function of inverse temperature for TBC confined in 15.6 and 7.4 nm CPG are given in Figs. 2 and 3. The results for bulk TBC obtained earlier [1, 2] are presented for comparison.

Similarly to the earlier results [1, 2] the ^{2}H spin-lattice relaxation times of TBC for both new sizes of CPG are insensitive to the liquid–solid I phase transition, however the ^{1}H T_1 data exhibit a small modification of the slope in the temperatures range corresponding to the solid phase I on the DSC curves.

Lowering the temperature, the plots of T_1 for both sizes of CPG exhibit discontinuities, which are associated with solid I – solid II transition manifesting also in the DSC measurements. This transition detected by proton and deuteron NMR relaxation times occurs at 205 K for 15.6 nm CPG and at about 183 K for 7.4 nm CPG. Taking into account that the confined systems always exhibit large transition temperature differences due to the broadening of transitions, the NMR results are in good agreement with the ones obtained from DSC method, 209 K and 183 K for 15.6 nm and 7.4 nm CPG, respectively.

In the temperature regions considered, the proton and deuteron T_1 relaxation time values of TBC confined in CPG are reduced. The reduction is larger for 7.4 nm pore size, showing increasing restriction of the translational motion and tumbling with the reduced pore size. These results are in agreement with previous observations [1, 2] and those given in literature [5, 6, 8].

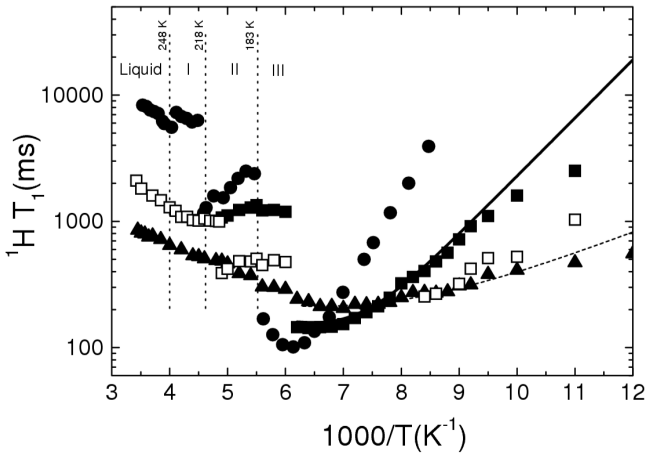

Fig. 2. Temperature dependences of ^{1}H relaxation time, T_1, for TBC confined in 15.6 nm CPG (open and solid squares for the two components of relaxation), in 7.4 nm CPG (solid triangles) and bulk TBC (solid circles).

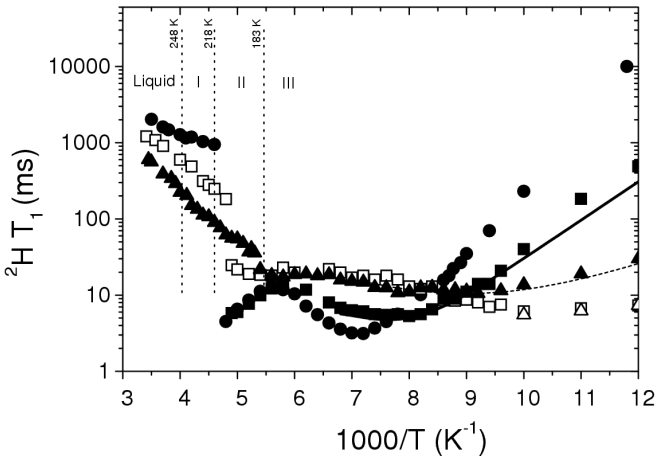

Fig. 3. Temperature dependences of ^{2}H relaxation time, T_1, for TBC confined in 15.6 nm CPG (open and solid squares for the two components of relaxation), in 7.4 nm CPG (open and solid triangles for the two components of relaxation) and bulk TBC (solid circles).

Below the temperature of the solid I – solid II phase transition of TBC confined to 15.6 nm CPG, two spin-lattice relaxation components are revealed by proton and deuteron data. The two-component system corresponds to two dynamically different regions formed as a result of confinement. One can be attributed to a more mobile fraction of molecules in the liquid-like surface layer and the other to the bulk-like phase at the center of the pore.

In temperatures between 165 K and 105 K, the two-exponential magnetization recovery of the proton relaxation disappears. The values of the proton relaxation times of both regions of confinement TBC are so similar that it is very difficult to distinguish between them.

For the 7.4 nm pore system in the temperature range studied only one component of the spin-lattice relaxation times of TBC was observed for the proton data, whereas the ^{2}H spin-lattice relaxation times show one component of T_1 above 100 K. It follows that the fast exchange limit is fulfilled and only a single exchange averaged T_1 is observed.

The bulk-like component of confined TBC in phase III in the plots of ^{1}H and ^{2}H spin-lattice relaxation times exhibit minima. The minima are higher, shallower, and wider for 7.4 nm than for 15.6 nm CPG and than in the bulk TBC. Broad minima have been associated with a distribution of correlation times as a consequence of the confinement. It is a result of coexistence of subphases within the bulk-like component with different correlation times characterizing rotation of the tert-butyl group.

^{1}H relaxation proceeds mainly via dipolar coupling, while ^{2}H relaxation is dominated by the quadrupolar interaction. As in the bulk TBC, both processes are modulated by a composite motion involving reorientation of the methyl groups about their symmetry axes (C_3 rotation) and rotation of the whole tert-butyl group about the axis of the C–Cl bond (C_3' reorientation). Assuming that the motions are thermally activated and independent of each other, the intra-methyl relaxation rate of protons and deuterons can be analyzed by the following expressions [30, 31]:

$$\left(\frac{1}{T_1^{1\mathrm{H}}}\right)^{\mathrm{ME}} = \frac{9}{80}\frac{\gamma^4\hbar^2}{r^6}\sum_{i=1}^{3} A_i(\theta,\varphi) f(\omega,\tau_i), \tag{1}$$

$$\left(\frac{1}{T_1^{2\mathrm{H}}}\right)^{\mathrm{ME}} = \frac{3}{50}\pi^2\left[\frac{2I+3}{I^2(2I-1)}\right]\chi^2\sum_{i=1}^{3} A_i(\theta,\varphi) f(\omega,\tau_i), \tag{2}$$

where all parameters have their usual meaning [1, 2].

It is sufficient to assume the existence of only two kinds of tert-butyl groups in bulk-like phase of TBC in both 15.6 and 7.4 nm CPG. The best fit of Eqs. (1) and (2), with the simple assumption that the tert-butyl groups are dynamically different, i.e. that the C_3' reorientation is described by different activation parameters, is shown by the solid and dashed lines in Figs. 2 and 3. An attempt to rationalize the relaxation results by fitting to different distribution models (like Cole-Cole, Cole-Davidson, Fuoss-Kirkwood [32]) has not been successful, even for the very broad and shallow minimum of TBC in 7.4 nm CPG.

The calculated activation energies and preexponential factors for the C_3' rotation in two dynamically different states of bulk-like phase, together with those earlier obtained for the bulk TBC, from both ^{1}H and ^{2}H T_1 data, are given in

TABLE II

Activation energies and the preexponential factors of the C_3' motion of bulk-like phase of TBC confined to 15.6 nm and 7.4 nm pore diameters CPG obtained from ^{1}H, ^{2}H T_1, and ^{2}H NMR spectra.

	^{1}HT_1		^{2}HT_1		^{2}H spectra	
	15.6 nm	7.4 nm	15.6 nm	7.4 nm	15.6 nm	7.4 nm
Subphase I						
E_a [kJ/mol]	8.8	4.2	9.6	4.6	9.3	4.6
τ_0 [s]	$3.5{\cdot}10^{-13}$	$1.4{\cdot}10^{-11}$	$4{\cdot}10^{-13}$	$2.2{\cdot}10^{-11}$	$4.8{\cdot}10^{-13}$	$1.26{\cdot}10^{-11}$
Subphase II						
E_a (kJ/mol)	8.8	4.2	9.6	4.6	7.8	4.4
τ_0 [s]	$0.2{\cdot}10^{-11}$	$1{\cdot}10^{-10}$	$0.9{\cdot}10^{-11}$	$1{\cdot}10^{-10}$	$0.18{\cdot}10^{-11}$	$1{\cdot}10^{-10}$
TBC in bulk [1]						
E_a [kJ/mol]	15.5					
τ_0 [s]	$1{\cdot}10^{-14}$					

Table II. Note that the contribution of the C_3 motion to the temperature dependence of T_1 at the discussed range is insignificant ($\tau_c(C_3) \gg \tau_c(C_3')$).

The derived activation energies considered in the context of the change induced by confinement effects are lower than in bulk for all molecular groups but taking into account preexponential factor values, the molecular motion of the tert-butyl groups is slower. The fact that the energies of the tert-butyl reorientation are much lower than in the bulk TBC and lower than for TBC confined to larger pore diameter [2], may result from a decrease of the intermolecular interactions in the bulk liquid phase of confined TBC. The slowing down of the motion can be due to the geometrical restrictions and is dependent on the degree of reduction of the pore width.

3.3. ^{1}H NMR lineshapes and linewidth

Figure 4 depicts the ^{1}H NMR lineshapes of bulk and confined TBC at different temperatures, while Fig. 5 shows the corresponding linewidths as a function of reciprocal temperature.

The linewidths of TBC in the liquid phase in both sizes of CPG are nearly temperature independent and compare to those for phase I of the bulk sample. It can be due to the restrictions of the translational motion and molecular tumbling responsible for T_2.

Below the freezing point, 204 K for 15.6 nm CPG and 192 K for 7.4 nm CPG, the line is composed of a narrower line superimposed on a broader one, suggesting two different molecular mobilities of the confined TBC. The broad component can be attributed to molecules of the crystalline solid localized at the center of the

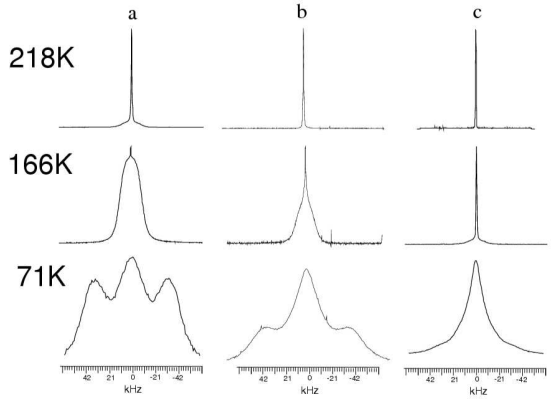

Fig. 4. ^{1}H line shapes of TBC confined (b) in 15.6 nm CPG and (c) in 7.4 nm CPG at different temperatures in comparing to (a) bulk TBC.

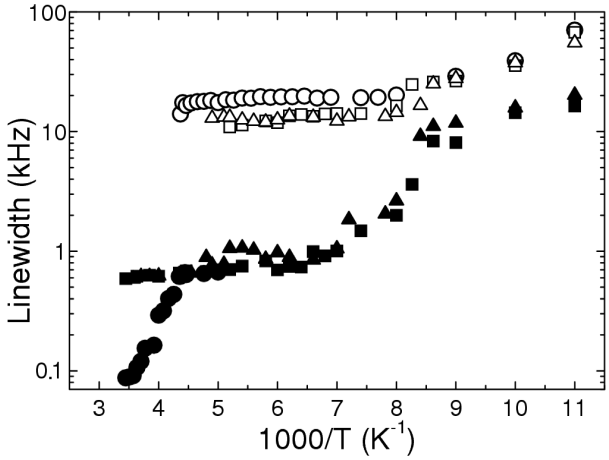

Fig. 5. Temperature dependences of ^{1}H linewidths for TBC confined in 15.6 nm (open and solid squares for the two spectral components), in 7.4 nm CPG (open and solid triangles for the two spectral components) and bulk TBC (open and solid circles for the two spectral components).

pores and the narrow line to a more mobile fraction of molecules in the liquid-like surface layer.

The linewidths of the narrow components of TBC confined in 15.6 and 7.4 nm CPG start to increase at 138 K and 151 K, respectively, reaching linewidths of broad component. The linewidths of the broad components are nearly constant up to 138 K and than grow continuously, reflecting the decreasing in the rate of the molecular reorientations C_3 and C_3'. We have made similar observations in previous investigations of TBC confined to other sizes CPG and other types of pores [1, 2].

3.4. ^2H NMR spectra

The temperature changes of the representative ^{2}H spectra of TBC confined to CPG of pore diameter 7.4 and 15.6 nm and those obtained in the bulk TBC, given for comparison, are shown in Fig. 6. One single narrow line is observed down to 206 K for 15.6 nm CPG and to 196 K for 7.4 nm CPG, reflecting the lowering of the freezing point of confined TBC by about 15 K and 27 K, respectively. Below the freezing, a narrow liquid-like component stemming from more mobile molecules, is still visible and is superimposed on the broad line with the quadrupolar splitting

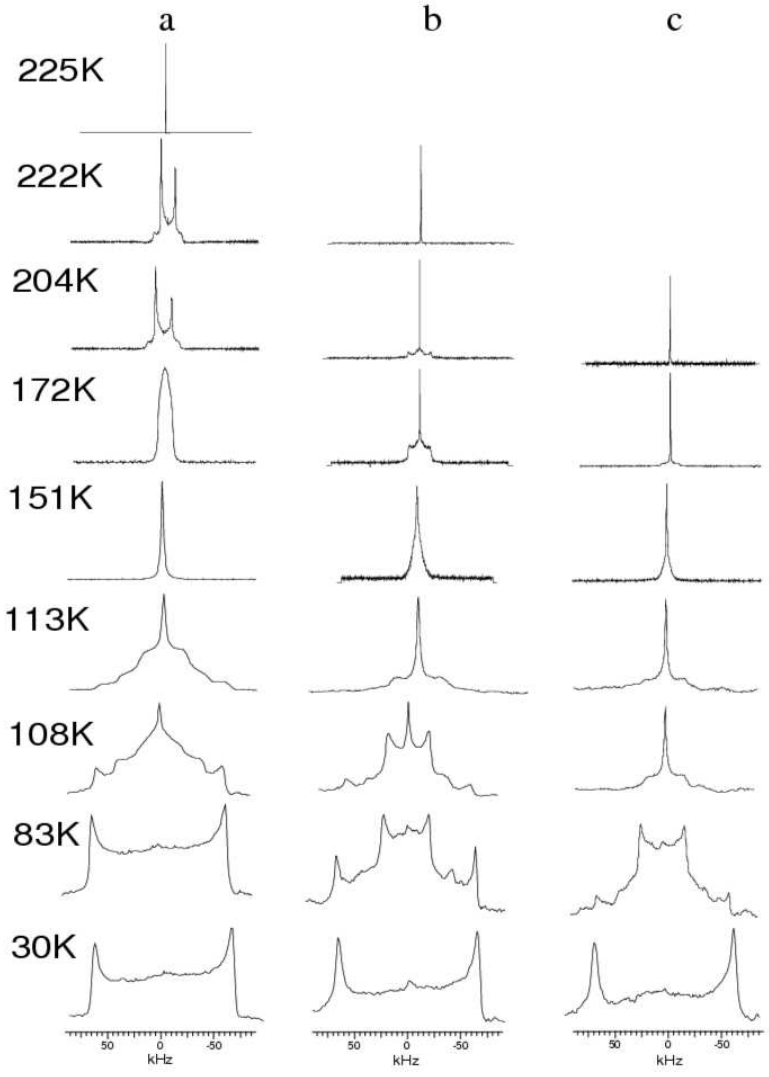

Fig. 6. The representative ^{2}H spectra of TBC confined to CPG of pore diameter (b) 15.6 nm and (c) 7.4 nm in comparison to (a) bulk TBC.

of 12.5 kHz, indicating that molecules perform fast methyl, C_3, and fast tert--butyl, C_3', rotations. In the smaller pores the intensity of the narrow component is predominant and is still visible until 90 K.

When temperature decreases, the spectra become the double Pake doublets with quadrupolar splittings of 40, 80, and 128 kHz. The molecules perform an intermediate to slow C_3 rotation and a fast C_3' rotation. Then the C_3' rotation is passing through the intermediate rate scale and finally at 30 K rotation of the tert-butyl group is stopped. TBC molecules become rigid on the R time scale as reflected in Fig. 6. The relative intensities of components attributed to the bulk-like phase of the confined TBC at the discussed temperature range are approximately equal to 0.5 and 0.2 for 15.6 nm and 7.4 nm CPG, respectively.

The parameters of molecular dynamics can be derived from simulations of the spectra. The representative simulated and experimental ^{2}H spectra of TBC confined to 15.6 nm and 7.4 nm CPG, in a temperature range of 111–70 K, are shown in Figs. 7 and 8. The spectra were calculated assuming superposition of three lines, which agrees with the results of T_1 analysis.

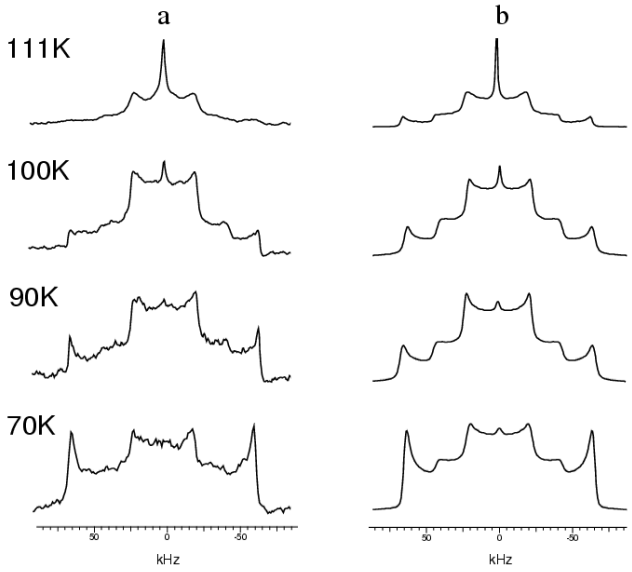

Fig. 7. Experimental (a) and simulated (b) ^{2}H NMR spectra of TBC confined to 15.6 nm CPG in the temperature range of 111–70 K.

The parameters used for the simulation were described previously [1, 2]. Activation energies and preexponential factors of the C_3' rotation rates of the two subgroups of TBC confined to 15.6 nm and 7.4 nm CPG, determined from the ^{2}H spectra simulations are shown in Table II. The obtained values are in good agreement with those calculated from T_1 data. The correlation times of C_3'

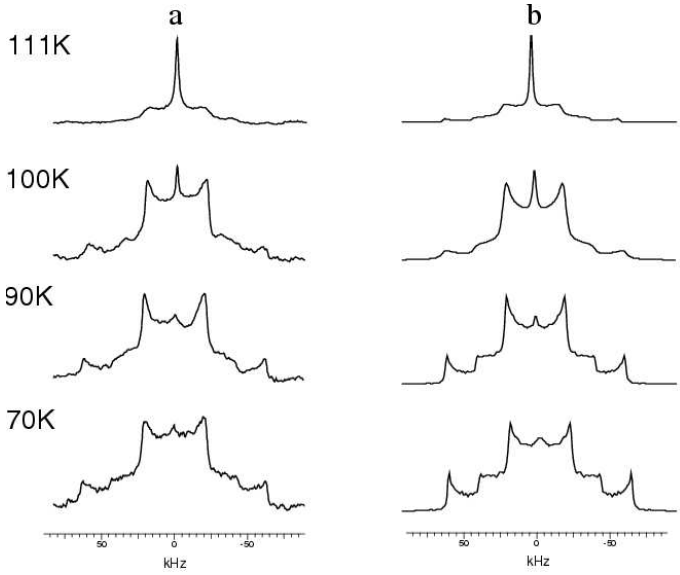

Fig. 8. Experimental (a) and simulated (b) ^{2}H NMR spectra of TBC confined to 7.4 nm CPG in the temperature range of 111–70 K.

rotation of molecules located at the surface-affected phase are longer than those characterizing any of the subphases of the bulk-like phase.

4. Conclusions

The results show that the depression of the phase transition temperature is the pore size dependent and also that the confinement has less influence on the transition to the plastic phase than on the freezing and on the solid II – solid III transition.

As a result of confinement, TBC forms a two-component system corresponding to two dynamically different regions: the surface-affected one, composed of molecules located at the pore surface, and the bulk-like phase located at the center of the pores. The bulk-like component of the confined TBC, in temperatures corresponding to phase III, is characterized by two dynamically different subphases. The tert-butyl group motion in both subphases is more restricted than in the bulk TBC, although the activation energies are lower.

The largest effect of confinement is observed in the case of the smaller pore diameter of the CPG studied, where a large fraction of confining molecules experiences direct contact with pore walls and large topological stress.

Acknowledgment

One of us (L. S.) wishes to acknowledge the financial support of the State Committee for Scientific Research under grant No. 3 T09A 127 26.

References

[1] L. Wasyluk, B. Peplinska, J. Klinowski, S. Jurga, *Phys. Chem. Chem. Phys.* **4**, 2392 (2002).

[2] L. Wasyluk, B. Peplinska, S. Jurga, *Solid State Nucl. Magn. Reson.* **25**, 177 (2004).

[3] R. Kimmich, F. Klammler, V.D. Skirda, I.A. Serebrennikova, A.I. Maklakov, N. Fatkullin, *Appl. Magn. Reson.* **4**, 425 (1993).

[4] V.S. Sullivan, Y.J. Kim, S. Xu, J. Jonas, J.P. Korb, *Langmuir* **15**, 4664 (1999).

[5] L. Gjerdaker, D.W. Aksnes, G.H. Sorland, M. Stocker, *Micoporous Mesoporous Mater.* **42**, 89 (2001).

[6] D.W. Aksnes, L. Gjerdaker, L. Kimtys, *J. Mol. Struc.* **522**, 209 (2000).

[7] H.F. Booth, J.H. Strange, *Mol. Phys.* **93**, 263 (1998).

[8] D.W. Aksnes, L. Gjerdaker, L. Kimtys, *J. Mol. Struc.* **509**, 297 (1999).

[9] E. Gedat, A. Schreiber, J. Albrecht, T. Emmler, I. Shenderovich, G.H. Findenegg, H.H. Limbach, G. Buntkowsky, *J. Phys. Chem. B* **106**, 1977 (2002).

[10] J. Bodurka, G. Buntkowsky, A. Gutsze, H.H. Limbach, *Z. Naturforsch.* **51**, 81 (1996).

[11] C.L. Jackson, G.B. Mckenna, *J. Chem. Phys.* **93**, 9002 (1990).

[12] G. Dosseh, D. Morineau, C. Alba-Simionesco, *J. Phys. IV* **10**, 99 (2000).

[13] K. Morishige, K. Kawano, *J. Chem. Phys.* **112**, 11023 (2000).

[14] E.R. Andrew, K. Jurga, E. Szczesniak, *Mol. Phys.* **65**, 1421 (1988).

[15] G.H. Penner, B.Y. Zhao, K.R. Jeffrey, *Z. Naturforsch. A* **50**, 81 (1995).

[16] J.A. Ripmeester, C.I. Ratcliffe, *J. Chem. Phys.* **82**, 1053 (1985).

[17] S. Urban, Z. Tomkowicz, J. Mayer, T. Waluga, *Acta Phys. Pol. A* **48**, 61 (1975).

[18] J.H. Davis, K.R. Jeffrey, M. Bloom, M.I. Valic, T.P. Higgs, *Chem. Phys. Lett.* **42**, 390 (1976).

[19] R. Kimmich, *NMR: Tomography, Diffusometry, Relaxometry*, Springer, Berlin 1997.

[20] M.S. Greenfield, A.D. Ronemus, R.L. Vold, R.R. Vold, P.D. Ellis, T.E. Raidy, *J. Magn. Reson.* **72**, 89 (1987).

[21] G. Dosseh, Y.D. Xia, C. Alba-Simionesco, *J. Phys. Chem. B* **107**, 6445 (2003).

[22] A. Ksiazczak, I. Nagata, *Thermochim. Acta* **254**, 31 (1995).

[23] R. Mu, V.M. Malhotra, *Phys. Rev. B* **44**, 4296 (1991).

[24] D. Morineau, G. Dosseh, C. Alba-Simionesco, P. Llewellyn, *Philos. Mag. B* **79**, 1847 (1999).

[25] P.E. Sokol, W.J. Ma, K.W. Herwig, W.M. Snow, Y. Wang, J. Koplik, J.R. Banavar, *Appl. Phys. Lett.* **61**, 777 (1992).

[26] P. Espeau, J.W. White, *J. Chem. Soc. Faraday Trans.* **93**, 3197 (1997).

[27] D.D. Awschalom, J. Warnock, *Phys. Rev. B* **35**, 6779 (1987).

[28] R. Mu, Y. Xue, D.O. Henderson, D.O. Frazier, *Phys. Rev. B* **53**, 6041 (1996).

[29] R. Mu, F. Jin, S.H. Morgan, D.O. Henderson, E. Silberman, *J. Chem. Phys.* **100**, 7749 (1994).

[30] M.B. Dunn, C.A. Mcdowell, *Mol. Phys.* **24**, 969 (1972).

[31] D.W. Aksnes, K. Ramstad, *Magn. Reson. Chem.* **27**, 830 (1989).

[32] P.A. Beckmann, *Phys. Rep.* **171**, 85 (1988).